



## Demonstration of InAsBi photoresponse beyond 3.5 $\mu\text{m}$

I. C. Sandall, F. Bastiman, B. White, R. Richards, D. Mendes, J. P. R. David, and C. H. Tan

Citation: *Applied Physics Letters* **104**, 171109 (2014); doi: 10.1063/1.4873403

View online: <http://dx.doi.org/10.1063/1.4873403>

View Table of Contents: <http://scitation.aip.org/content/aip/journal/apl/104/17?ver=pdfcov>

Published by the [AIP Publishing](http://aip.org)

---

### Articles you may be interested in

[Demonstration of shortwavelength infrared photodiodes based on type-II InAs/GaSb/AlSb superlattices](#)

*Appl. Phys. Lett.* **100**, 211101 (2012); 10.1063/1.4720094

[High-performance type-II InAs/GaSb superlattice photodiodes with cutoff wavelength around 7  \$\mu\text{m}\$](#)

*Appl. Phys. Lett.* **86**, 091109 (2005); 10.1063/1.1879113

[Solar-blind ultraviolet photodetectors based on superlattices of AlN/AlGa\(In\)N](#)

*Appl. Phys. Lett.* **82**, 1323 (2003); 10.1063/1.1557325


[Investigation of trap-assisted tunneling current in InAs/\(GaIn\)Sb superlattice long-wavelength photodiodes](#)

*Appl. Phys. Lett.* **81**, 4757 (2002); 10.1063/1.1529306





[InGaAsSb thermophotovoltaic diode: Physics evaluation](#)

*J. Appl. Phys.* **85**, 2247 (1999); 10.1063/1.369533

---



## Instruments for Advanced Science

 <p><b>Gas Analysis</b></p> <ul style="list-style-type: none"><li>dynamic measurement of reaction gas streams</li><li>catalysis and thermal analysis</li><li>molecular beam studies</li><li>dissolved species probes</li><li>fermentation, environmental and ecological studies</li></ul>	 <p><b>Surface Science</b></p> <ul style="list-style-type: none"><li>UHV TPD</li><li>SIMS</li><li>end point detection in ion beam etch</li><li>elemental imaging - surface mapping</li></ul>	 <p><b>Plasma Diagnostics</b></p> <ul style="list-style-type: none"><li>plasma source characterization</li><li>etch and deposition process reaction</li><li>kinetic studies</li><li>analysis of neutral and radical species</li></ul>	 <p><b>Vacuum Analysis</b></p> <ul style="list-style-type: none"><li>partial pressure measurement and control of process gases</li><li>reactive sputter process control</li><li>vacuum diagnostics</li><li>vacuum coating process monitoring</li></ul>
--	---	---	---

Contact Hiden Analytical for further details:  
[www.HidenAnalytical.com](http://www.HidenAnalytical.com)  
[info@hiden.co.uk](mailto:info@hiden.co.uk)  
**CLICK TO VIEW** our product catalogue

## Demonstration of InAsBi photoresponse beyond 3.5 $\mu\text{m}$

I. C. Sandall,<sup>a)</sup> F. Bastiman, B. White, R. Richards, D. Mendes, J. P. R. David, and C. H. Tan  
*Department of Electronic and Electrical Engineering, The University of Sheffield, Sir Frederick Mappin Building, Mappin Street, Sheffield S1 3JD, United Kingdom*

(Received 31 October 2013; accepted 10 April 2014; published online 30 April 2014)

An Indium Arsenide Bismide photodiode has been grown, fabricated, and characterized to evaluate its performance in the Mid Wave Infrared region of the spectrum. Spectral response from the diode has been obtained up to a diode temperature of 225 K. At this temperature, the diode has a cut off wavelength of 3.95  $\mu\text{m}$ , compared to 3.41  $\mu\text{m}$  in a reference Indium Arsenide diode, indicating that Bismuth has been incorporated to reduce the band gap of Indium Arsenide by 75 meV. Similar band gap reduction was deduced from the cut off wavelength comparison at 77 K. From the dark current data, shunt resistance values of 8 and 39  $\Omega$  at temperatures of 77 and 290 K, respectively, were obtained in our photodiode. © 2014 Author(s). All article content, except where otherwise noted, is licensed under a Creative Commons Attribution 3.0 Unported License. [<http://dx.doi.org/10.1063/1.4873403>]

The Mid Wave Infrared (MWIR) spectral region between 3.0 and 5.0  $\mu\text{m}$  is of great interest for a number of applications including military imaging,<sup>1</sup> gas and biological sensing.<sup>2</sup> Currently, the best performing photodiodes operating over this spectral region are realized using Cadmium Mercury Telluride (CMT), Indium Antimony (InSb), and Lead Selenide (PbSe), while type-II superlattices (such as  $\text{In}_x\text{Ga}_{1-x}\text{Sb}/\text{InAs}$  and  $\text{InAs}/\text{InAs}_{1-x}\text{Sb}_x$ ) are rapidly improving. PbSe is not available in large format arrays while InSb and CMT require aggressive cooling to achieve high performance. The bandgap of CMT can be tuned via its composition<sup>3,4</sup> to allow it to access the MWIR region. However, CMT is an expensive and difficult semiconductor to grow and fabricate, limiting both the price and quantity of devices that are available. Type-II superlattices have also been demonstrated as photodiodes operating in the 3–5  $\mu\text{m}$  range,<sup>5,6</sup> but good performance was only obtained at low temperatures due to the complexity of the growth and issues with fabricating type-II superlattices with low surface currents.

Over recent years, Indium Arsenide (InAs) has attracted renewed interest as it has been demonstrated to operate as an excellent avalanche photodiode with single carrier (electron) multiplication and low excess noise.<sup>7,8</sup> Furthermore, the growth and fabrication has been developed to provide highly uniform wafers with low dark currents.<sup>9–11</sup> Unfortunately, InAs has a cutoff wavelength of 3.5  $\mu\text{m}$  and is not suitable for various MWIR applications. One possibility to reduce the bandgap and, hence, extend the detection wavelength is to utilize the alloy Indium Arsenide Antimonide (InAsSb), which has the potential to reach wavelengths of  $\sim 10 \mu\text{m}$  due to its bowing parameter.<sup>12</sup> To grow thick bulk layers with a sufficiently high Sb concentration would require sophisticated buffer layers to be grown to alleviate the large lattice mismatch. Commercially available InAsSb diodes can detect up to a wavelength of 5.8  $\mu\text{m}$ . An alternative approach would be to make use InAs and Indium Bismide (InBi) to grow dilute-Bismuth containing InAs. Indium Arsenide Bismide

(InAsBi) layers have previously been grown, and the photoluminescence results suggested that a bandgap reduction of 55 meV per 1% of Bi can be obtained.<sup>13–15</sup> However, Molecular Beam Epitaxy (MBE) growth of such layers has proven to be difficult due to the large miscibility gap of InAs and InBi,<sup>14</sup> requiring low growth temperatures ( $< 400^\circ\text{C}$ ) and near stoichiometric flux ratios.<sup>13</sup> Even when great care is taken to maintain constant sample temperatures and constant fluxes throughout growth, the InAsBi layers grown have shown evidence of non-uniformity and phase separation.<sup>13</sup> In this work, we report the growth and fabrication that have produced a promising InAsBi MWIR photodiode operating at Peltier cooler compatible temperatures.

The sample was grown in an Omicron molecular beam epitaxy-scanning tunneling microscope (MBE-STM). For the Bismuth containing layers, the In, As<sub>4</sub>, and Bi fluxes were 5.0, 8.0, and  $3.0 \pm 0.1$  atoms/nm<sup>2</sup>/s, respectively. The sample was grown on an n+ InAs substrate and comprised a 1000 nm n-doped InAs layer ( $1 \times 10^{18} \text{ cm}^{-3}$  of Si) grown at 500 °C, followed by a 1000 nm intrinsic region which was formed by ten periods of 90 nm  $\text{InAs}_{0.98}\text{Bi}_{0.02}$  wells separated by 10 nm InAs barriers to remove Bi from the super-saturated surface and near-surface layers grown at  $\sim 350^\circ\text{C}$ . The sample was then capped with a 1000 nm p+ InAs layer ( $1 \times 10^{18} \text{ cm}^{-3}$  of Be) grown at 500 °C. The InAs barriers were included in the sample structure to prevent the accumulation of Bi on the sample surface during growth. Svensson *et al.*<sup>13</sup> showed that non-stoichiometric InAsBi growth could result in In droplets on the surface, while Bastiman *et al.*<sup>16</sup> showed that excess Bi flux could cause Bi droplets to form on GaAsBi surfaces. In our first growth campaign that aimed to demonstrate an InAsBi device, we employed a coarse optimization of the As and Bi fluxes that prevented surface droplet formation by incorporating the excess surface Bi into the lattice by periodically growing nominally pure InAs. It has recently been shown that the Bi surface lifetime on a static GaAs surface is significantly longer than the monolayer growth time used in this work,<sup>17</sup> so merely halting growth periodically is likely not enough to prevent the accumulation of Bi on the growth surface. For

<sup>a)</sup>[i.sandall@sheffield.ac.uk](mailto:i.sandall@sheffield.ac.uk)



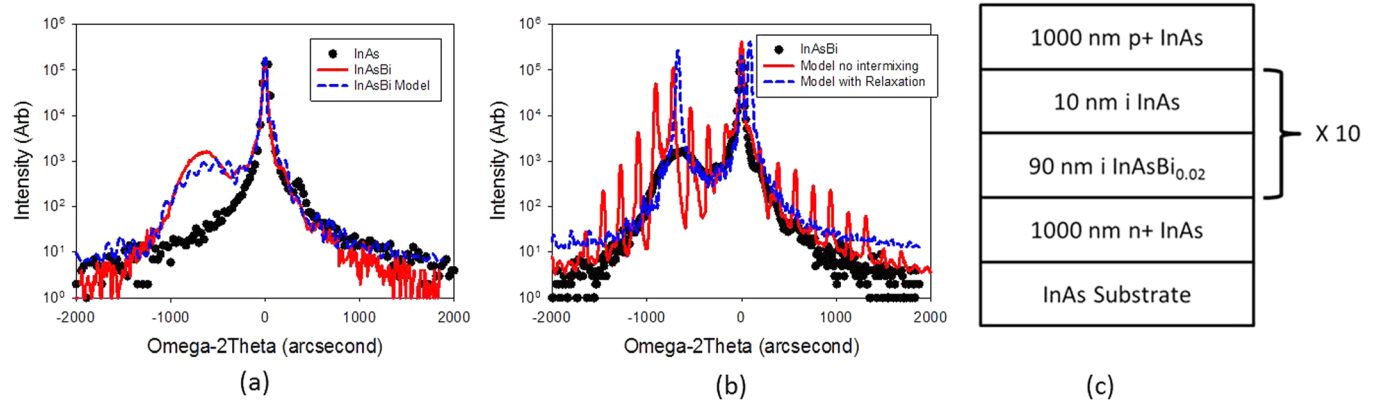


FIG. 1. (a) XRD spectra for InAs (symbols) and InAsBi (line) samples along with theoretical prediction for InAsBi (dashed line), (b) XRD spectra for the InAsBi sample along with theoretical predictions showing effects of no intermixing in the barriers (line) and under partial relaxation (dashed lines), (c) schematic of structure layers.

comparison purposes, an InAs pin was also grown with a 1000 nm thick p, i, and n layers all grown at 500 °C and with the same doping concentrations as the Bi containing sample.

High resolution [004]  $\theta$ - $2\theta$  X-ray Diffraction (XRD) scans were performed on both the samples using a Bruker D8 Discover with the Cu  $K\alpha_1$  line. The resultant curves are shown in Figure 1(a). A clear secondary peak can be seen in the InAsBi sample suggesting successful incorporation of Bi. To estimate the percentage of Bi in the alloy, simulation of the XRD spectrum was performed using RADS Mercury software. In our simulations, the lattice constant and strain are the main unknown parameters. The empirical lattice constant of tetragonal InBi has been determined;<sup>18,19</sup> however, Zinc Blend-InBi (ZB-InBi) has not been synthesized. There are uncertainties in the theoretically predicted lattice constant of ZB-InBi, with values ranging from 6.5 to 7.02 Å reported in the literature.<sup>20–23</sup> The simulated XRD curve shown in Figure 1(a) was modelled with a lattice constant of 7.02 Å and 1.7% of Bi, without the inclusion of the InAs barriers, and assuming the InAsBi layer to be fully strained. The barriers are not likely to be pure InAs as recent results have shown that the Bi composition of similar GaAs barriers in GaAsBi growth only drops to about half that of the GaAsBi regions.<sup>24</sup> This is further supported by the lack of superlattice peaks in the XRD spectrum. Such peaks can clearly be seen in the simulated curve when the periodic variation in the Bi content due to the spacer layers is included (Figure 1(b)), in this simulation we have considered the i-region to consist of ten 90 nm thick InAsBi wells separated by 10 nm InAs barriers, as initially designed. Assuming a fully strained system, the percentage Bi of 1.7% to 3.6% was obtained for the range of lattice constants from 7.02 to 6.5 Å, as summarized in Table I.

To further analyze the effect of strain, we also performed the XRD simulations for a partially relaxed system, as shown in Figure 1(b), here we have assumed a 30% relaxation in the first InAsBi well and at the p+ cap. For the partially relaxed simulation, we clearly observe a second positively offset peak, we observe a similar peak for any degree of relaxation. The lack of this positively offset peak in the measured XRD suggests that the InAsBi is pseudomorphically strained, although we are unable to determine the relative amount of strain, or totally discount the

possibility of strain relaxation, without a more detailed reciprocal space map which is beyond the scope of this paper.

Given the range of potential lattice constants and the uncertainty in the strain of the InAsBi layer, it is a non-trivial task to determine the Bi concentration. Table I gives the range of potential Bi concentrations based upon the possible ZB-InBi lattice constants, and, assuming a fully strained or fully relaxed system, although, as mentioned previously, due to the lack of a tensile InAs peak in the XRD, the fully relaxed values are merely an upper limit at each lattice constant.

Both samples were fabricated into circular mesa diodes (with radii ranging from 50 to 200  $\mu\text{m}$ ) using standard mask lithography and were then etched using our preferred chemical etching procedures for InAs of a 1:1:1 (phosphoric acid: hydrogen peroxide: de-ionized water) etch, followed by a finishing etch of 1:8:80 (sulphuric acid: hydrogen peroxide: de-ionized water).<sup>7</sup> For the InAsBi sample, an additional finishing etch comprising a rinse in 2:3 (hydrochloric acid: Isopropyl alcohol (IPA)) followed by a 3 s anneal at 340 °C was used. This additional step was included to try and obtain clean As rich surfaces<sup>25</sup> and suppress surface leakage currents. Ti/Au top contacts with thicknesses of 20/200 nm were deposited, and a common back n contact was formed from an identical layer of Ti/Au. The samples were then cleaved and mounted onto TO-5 headers, and the samples were secured into a Helium cooled cryostat for the measurements.

Current-Voltage (IV) characteristics of the InAsBi diode were measured by connecting the sample to a Keithley Source Measure Unit (SMU) with a compliance current of 10 mA, the resultant traces for a device with a radius of 100  $\mu\text{m}$  are shown in Figure 2.

At room temperature, the InAsBi sample shows very high reverse leakage current. However, at 250 K and lower

TABLE I. Range of possible Bi concentrations based on various reported lattice constants and assuming a fully strained or fully relaxed system.

References	InBi lattice constant (Å)	Fully relaxed	Fully strained
1	6.5	7.4	3.6
2	6.64	5.7	2.7
3	6.686	5.2	2.6
4	7.02	3.4	1.7

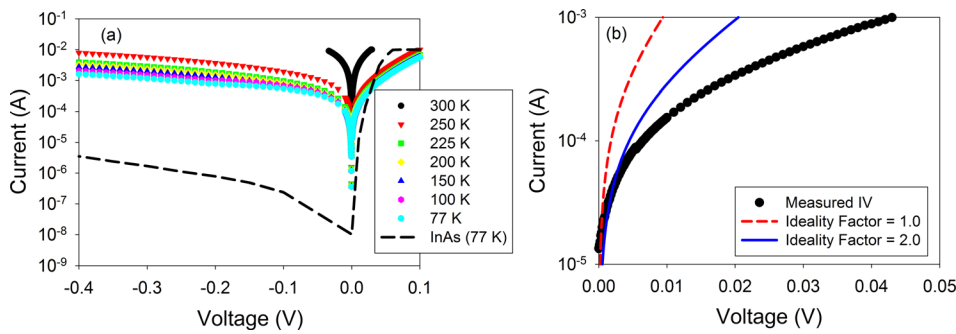


FIG. 2. (a) Current-Voltage measurements at various temperatures for InAsBi sample (symbols) and the InAs reference sample (dashed line) and (b) Low voltage forward IV characteristics at 77 K, (symbols) and fittings with different ideality factors (lines).

temperatures, a diode like characteristic was observed with a turn on voltage around 20 mV (corresponding to 10 mA). This turn on voltage is larger than that of the InAs reference sample (dashed line in Figure 2(a)), contrary to a smaller value expected from the reduced bandgap of InAsBi. To investigate this discrepancy, we have determined the ideality factor of the diode and found it to be close to 2 at very low values of forward bias ( $<0.005$  V), however, at higher biases, the measured IVs deviate from the predicted curve (even with an ideality factor greater than 2) and produces a poor agreement (Figure 2(b)). This suggests that at lower biases, there is a significant amount of generation-recombination due to Shockley-Read-Hall processes, but, at higher voltages, the diode is limited due to a very high series resistance. At the moment, we are unable to determine the origin of this series resistance, but believe it is most likely due to unoptimized doping in the cladding layers or from a high contact resistance.

As the temperature was reduced from 290 to 250 K, a sharp reduction in the reverse dark current was obtained. A much more gradual reduction was measured as the temperature was further reduced from 250 to 77 K. From measurements on different sized mesas (not shown here), the dark current does not scale with area. Therefore, it is concluded that at all temperatures, the current still has a large surface current component. The dark currents for the InAs reference sample are significantly lower (over two orders of magnitude lower at 0 V than the InAsBi sample) and are bulk-like at room temperature. However, the InAs currents are still higher than the best reported InAs diodes<sup>7,9</sup> (by around 2 orders of magnitude at 290 K), indicating that the growth of both structures could be refined. By developing improved fabrication and passivation procedures, it should be possible to significantly reduce the dark currents in the InAsBi diodes, by suppressing the surface components. A similar issue was discovered with early InAs photodiodes,<sup>7</sup> however, with successful suppression of surface currents, the bulk dark current has been shown to be  $\sim 100$  times smaller.<sup>9</sup> To evaluate the electrical performance of the InAsBi diode, we have determined the shunt resistance by taking the differential of the IV curve at 0 V, yielding values of 8 and 39  $\Omega$  at 77 and 295 K, respectively. Similar values were obtained (within 10% of these) when the shunt resistance was calculated for different sized mesa diodes. These values are comparable with other MWIR detectors, including commercially available InAsSb (typically 5–20  $\Omega$  at room temperature), HgCdTe ( $\sim 0.9 \Omega$  at 140 K with a cut-off wavelength of 4.8  $\mu\text{m}$ ),<sup>26</sup> and type-II superlattices (140  $\Omega$  at 77 K with a cut off wavelength of 4.9  $\mu\text{m}$ ).<sup>27</sup>

Spectral measurements were obtained using a Varian 7000 Fourier Transform Infrared Spectrometer coupled with a Stanford Research (SR570) current pre-amplifier. The normalized spectral response of the InAsBi sample at 0 V bias, at various temperatures, is shown in Figure 3(a). Due to the large increase in dark current above 225 K, it was not possible to measure the spectra accurately above this temperature. The small shift in the atmospheric absorption features is thought to be due to measurement errors caused by the high dark current from the diodes.

As the temperature was increased, the cut off wavelength (defined as 50% intensity of the peak wavelength) of the InAsBi shifts to longer wavelength, with a longest cut off wavelength of 3.95  $\mu\text{m}$  being observed at 225 K. Figure 3(b) compares the spectral response of the InAs reference sample with the InAsBi sample at 225 K. Clearly, InAsBi has a longer cutoff wavelength compared to the InAs reference diode. The increase in wavelength for the InAsBi sample corresponds to a 75 meV reduction of the bandgap from InAs. This reduction is also deduced from the two samples at 77 K in Figure 3(c). Assuming that the reduction in bandgap with Bi incorporation is 55 meV/% as proposed in Ref. 13, this would indicate a Bi composition of  $\sim 1.5\%$ . Although this value lies outside of the range of concentrations simulated in Table I, it is close to the value of 1.7% calculated for a fully strained system with the largest lattice constant (7.02  $\text{\AA}$ ), ignoring the effect of the InAs spacer layers. Furthermore, it is worth bearing in mind that there are a number of other variables in the XRD modelling which could influence this result, as well as the fact that we have determined the shift in bandgap from photocurrent measurements while using data from an independent PL study to calibrate the wavelength shift to a Bismuth concentration. This result is the highest reported incorporation of Bi into an InAs photodiode.

The temperature dependence of the bandgap of InAsBi has been determined by calculating the dependence of the cut off wavelength, with the resultant photon energy versus temperature plots shown in the inset to Figure 3(a) for both InAs and InAsBi. The temperature dependence of the InAsBi sample was found to be 0.19 meV/K which is considerably smaller than that of InAs, 0.31 meV/K. This reduction in temperature sensitivity is greater than that which has been observed in GaAsBi,<sup>28,29</sup> where a reduction from 0.56 meV/K for GaAs to 0.4 meV/K was observed<sup>22</sup> when a comparable amount of Bi was added. In GaAsBi, this reduced temperature dependence has been attributed to an increase in localized states due to Bi clustering. It is likely that a similar mechanism is responsible



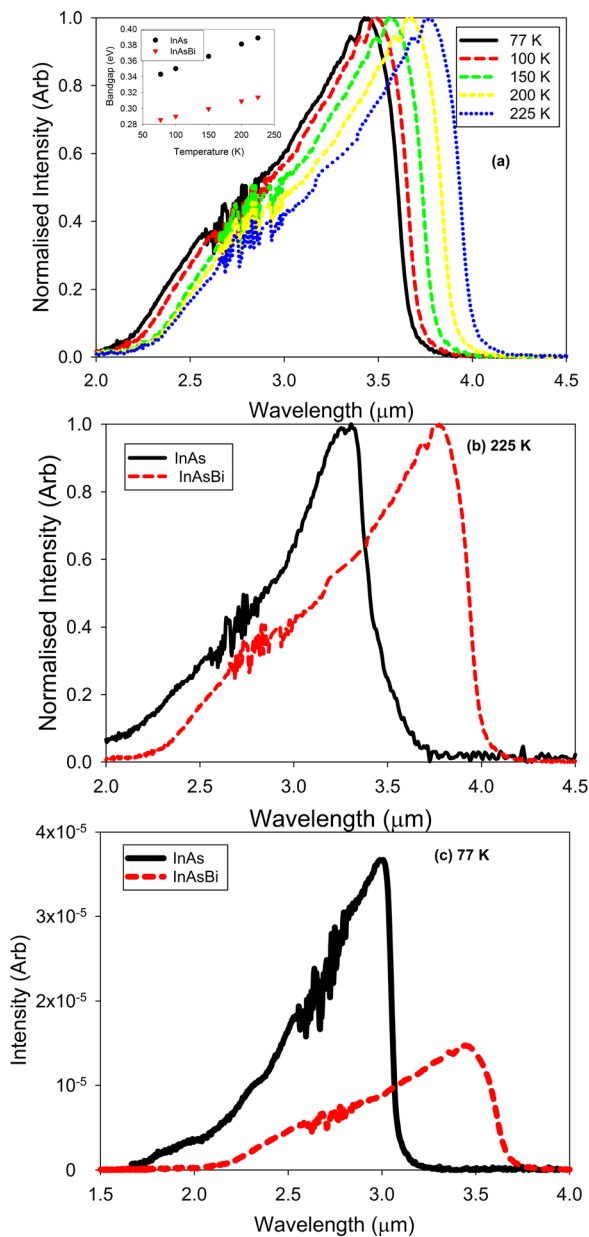


FIG. 3. (a) Spectral response of InAsBi sample with 0 V bias at various temperatures, the inset shows the temperature dependence of the band gap for both InAs and InAsBi, and comparisons of the spectral response of InAs and InAsBi at 225 K (b) and 77 K (c).

for the reduced temperature sensitivity observed here. However, given the reduced temperature sensitivity, compared to GaAs, it would appear that there is increased Bi clustering in InAsBi. Whether this is an intrinsic property of Bi inclusion in InAs or due to the relative immaturity of InAsBi growth is unclear and will require future investigation.

To investigate if the InAs p+ cap influences the spectral data in Figure 3, the measurements were repeated for the InAsBi sample with a 3–5  $\mu\text{m}$  filter which was used to remove any second order absorption at short wavelengths. The spectra at 77 K for both the InAs and the InAsBi are shown in Figure 4. The InAs sample only shows a very small tail of absorption at these longer wavelengths, indicating that the absorption measured for the InAsBi sample is not influenced by the p+ InAs cap.

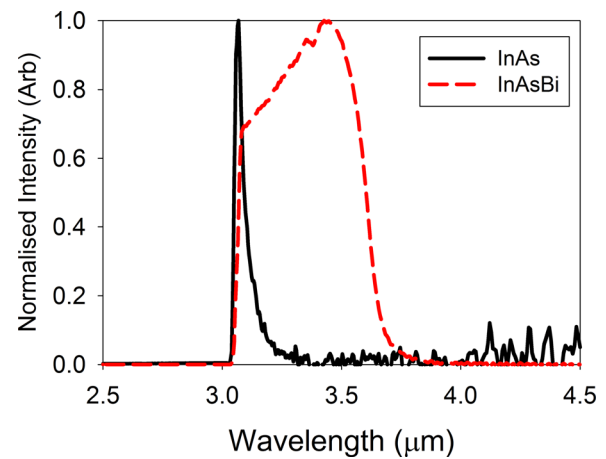


FIG. 4. 77 K Spectral response for InAs and InAsBi samples at 0 V bias in the presence of a 3–5  $\mu\text{m}$  filter.

These results illustrate that InAsBi has the potential to be utilized as a detector in the MWIR spectral region. While the thickness and composition of the Bi containing layers have been limited in this work due to strain build up across the device, this could be improved upon in future by utilizing InGaAs barriers to compensate the strain and potentially improve the performance. Further work is also required to further understand the properties and growth of InBi to allow the realization of high quality devices containing InAsBi. A second route to exploit InAsBi detectors would be to grow InAsBi on GaSb substrate to reduce lattice mismatch so that thicker InAsBi can be grown for higher detection efficiency in the MWIR, and possibly longer wavelengths.

In conclusion, we have grown, fabricated, and characterized an InAsBi containing photodiode with a Bi composition of around 1.5%. This leads to a cutoff wavelength of 3.95  $\mu\text{m}$  at a temperature of 225 K, along with the measurement of encouraging dark currents, given the relative immaturity of the material growth and fabrication. We have measured a reduced temperature dependence of the bandgap when compared to InAs.

- <sup>1</sup>I. Baker, S. Duncan, and J. Copley, *Proc. SPIE* **5406**, 133 (2004).
- <sup>2</sup>A. Krier, H. H. Gao, and Y. Mao, *Semicond. Sci. Technol.* **13**, 950 (1998).
- <sup>3</sup>S. Ghosh, S. Mallick, K. Banerjee, S. Velicu, J. Zhao, E. Plis, S. Krishna, and D. Silversmith, *J. Electron. Mater.* **37**, 1764 (2008).
- <sup>4</sup>V. I. Stafeev, K. O. Boltar, I. D. Burlakov, V. M. Akimov, E. A. Klimanov, L. D. Saginov, V. N. Solyakov, N. G. Mansvetov, V. P. Ponomarenko, A. A. Timofeev, and A. M. Filachev, *Semiconductors* **39**, 1215 (2005).
- <sup>5</sup>H. S. Kim, E. Plis, A. Khoshakhlagh, S. Myers, N. Gautam, Y. D. Sharma, L. R. Dawson, S. Krishna, S. J. Lee, and S. K. Noh, *Appl. Phys. Lett.* **96**, 033502 (2010).
- <sup>6</sup>J. V. Li, C. J. Hill, J. Mumolo, S. Gunapala, S. Mou, and S. L. Chuang, *Appl. Phys. Lett.* **93**, 163505 (2008).
- <sup>7</sup>A. R. J. Marshall, C. H. Tan, M. J. Steer, and J. P. R. David, *Appl. Phys. Lett.* **93**, 111107 (2008).
- <sup>8</sup>A. R. J. Marshall, P. Vines, P. J. Ker, J. P. R. David, and C. H. Tan, *IEEE J. Quantum Electron.* **47**, 858 (2011).
- <sup>9</sup>S. J. Maddox, W. Sun, Z. Lu, H. P. Nair, J. C. Campbell, and S. R. Bank, *Appl. Phys. Lett.* **101**, 151124 (2012).
- <sup>10</sup>P. J. Ker, A. Marshall, A. Krysa, J. P. R. David, and C. H. Tan, *IEEE J. Quantum Electron.* **47**, 1123 (2011).
- <sup>11</sup>I. Sandall, S. Zhang, and C. H. Tan, *Opt. Express* **21**, 25780 (2013).

- <sup>12</sup>G. Belenky, D. Wang, Y. Lin, D. Donetsky, G. Kipshidze, L. Shterengas, D. Westerfeld, W. L. Sarney, and S. P. Svensson, *Appl. Phys. Lett.* **99**, 141116 (2011).
- <sup>13</sup>S. P. Svensson, H. Hier, W. L. Sarney, D. Donetsky, D. Wang, and G. Belenky, *J. Vac. Sci. Technol. B* **30**, 02B109 (2012).
- <sup>14</sup>K. Y. Ma, Z. M. Fang, D. H. Jaw, R. M. Cohen, G. B. Stringfellow, W. P. Kosar, and D. W. Brpwn, *Appl. Phys. Lett.* **55**, 2420 (1989).
- <sup>15</sup>S. J. Maddox, H. P. Nair, V. D. Dasika, E. M. Krivoy, R. Salas, and S. R. Bank, in International Symposium on Compound Semiconductors (ISCS), Santa Barbara, CA, August 2012.
- <sup>16</sup>F. Bastiman, A. R. Mohamad, J. S. Ng, J. P. R. David, and S. J. Sweeney, *J. Cryst. Growth* **338**, 57 (2012).
- <sup>17</sup>R. D. Richards, F. Bastiman, C. J. Hunter, D. Mendes, A. R. Mohamad, J. S. Roberts, and J. P. R. David, *J. Cryst. Growth* **390**, 120 (2014).
- <sup>18</sup>K. Takano and T. Sato, *Phys. Lett. A* **44**, 309 (1973).
- <sup>19</sup>V. Degtyareva, M. Winzenick, and W. Holzappel, *Phys. Rev. B* **57**, 4975 (1998).
- <sup>20</sup>H. Okamoto and K. Oe, *Jpn. J. Appl. Phys., Part 1* **37**, 1608 (1998).
- <sup>21</sup>S. A. Barnett, *J. Vac. Sci. Technol. A* **5**, 2845 (1987).
- <sup>22</sup>A. Janotti, S.-H. Wei, and S. B. Zhang, *Phys. Rev. B* **65**, 115203 (2002).
- <sup>23</sup>K. Y. Ma, Z. M. Fang, R. M. Cohen, and G. B. Stringfellow, *J. Appl. Phys.* **68**, 4586 (1990).
- <sup>24</sup>C. J. Hunter, F. Bastiman, A. R. Mohamad, R. D. Richards, R. Beanland, and J. P. R. David, "Growth and characterization of bulk GaAsBi/GaAs p-i-n diodes," *J. Cryst. Growth* (submitted).
- <sup>25</sup>O. E. Tereshchenko, D. Paget, P. Chiaradia, J. E. Bonnet, F. Wiame, and A. Taleb-Ibrahimi, *Appl. Phys. Lett.* **82**, 4280 (2003).
- <sup>26</sup>J. B. Varesi, R. E. Bornfreund, A. C. Childs, W. A. Radford, K. D. Maranowski, J. M. Peterson, S. M. Johnson, L. M. Giegerich, T. J. de Lyon, and J. E. Jensen, *J. Electron. Mater.* **30**, 566 (2001).
- <sup>27</sup>C. Cervera, J. B. Rodriguez, R. Chaghi, H. Ait-Kaci, and P. Christol, *J. Appl. Phys.* **106**, 024501 (2009).
- <sup>28</sup>A. R. Mohamad, F. Bastiman, J. S. Ng, S. J. Sweeney, and J. P. R. David, *Appl. Phys. Lett.* **98**, 122107 (2011).
- <sup>29</sup>S. Francoeur, M. J. Seong, A. Mascarenhas, S. Tixier, M. Adamcyk, and T. Tiedje, *Appl. Phys. Lett.* **82**, 3874 (2003).